ELSEVIER

Journal of Alloys and Compounds 227 (1995) 10–17

Journal of ALLOYS AND COMPOUNDS

Structure determination of γ'-Fe_4N and ϵ-Fe_3N ☆

H. Jacobs, D. Rechenbach, U. Zachwieja

Fachbereich Chemie der Universität Dortmund, 44221 Dortmund, Germany

Received 19 December 1994; in final form 13 February 1995

Abstract

Single crystals of γ'-Fe_4N were prepared by high pressure ammonolysis. Our earlier published results (H. Jacobs and J. Bock, *J. Less-Common Met., 134* (1987) 215) differ from those which are now reported. γ'-Fe_4N crystallizes in the $CaTiO_3$ (perovskite) structure type: X-ray single-crystal diffractometer data, space group $Pm\bar{3}m$, $Z=1$ and $a=3.7900(6)$ Å, R/R_w $(w=1)=0.017/0.023$, $N(F_o^2) \geqslant 3\sigma(F_o^2)=59$ and $N(\text{var})=6$. Powder samples of ϵ-Fe_3N were prepared in a technical furnace. The crystal structure was studied by neutron powder diffraction at 9 K, room temperature and 609 K. ϵ-Fe_3N crystallizes in a hexagonal structure type: space group $P6_322$, $Z=2$, $a=4.6982(3)$ Å and $c=4.3789(3)$ Å, $N(F_o)=34$ and 5 structural parameters refined, $R_{\text{Profile}}=4.43\%$, $R_{\text{Bragg}}=4.14\%$ for the measurement at room temperature.

Keywords: Structure determination; Neutron powder diffraction; High pressure ammonolysis

1. Introduction

Iron nitrides are of fundamental importance for steel production and steel hardening. Details of reactions are presently unknown, and for example structural information is required to obtain reproducible qualities of the hardened steel surface [1]. The preparation of single crystals and single-phase samples is difficult because of the low thermal stability and high decomposition pressure of nitrogen at moderate temperatures [2]. Our investigations show, for example, for α-Fe/γ'-Fe_4N an N_2 pressure higher than 430 bar (limited by the apparatus used) at 450 °C. Decomposition of ϵ-Fe_3N into elements begins at about 400 °C.

In previous studies the crystal structures of phases of the iron–nitrogen system were often investigated with partially different results obtained [3–5]. Very detailed investigations were carried out by Jack in the 1940s and 1950s [6–8]. In general the structures were described correctly. Based on a close-packed arrangement of iron atoms, the nitrogen atoms occupy (if possible) corner-sharing octahedra. Up to now there have been no papers concerning structure solutions based on single-crystal data except [9], or based on refined powder diffraction data (X-ray or neutron).

2. Synthesis and structure of γ'-Fe_4N

Single crystals of γ'-Fe_4N were prepared for the first time by reaction of iron powder (Iron "reinst" DAB 6, E. Merck, Darmstadt, Germany) with supercritical ammonia ($p(NH_3)=6$–8 kbar, in the temperature range 460–580 °C) in high pressure autoclaves [10] with about 3 mol% FeI_2 ("wasserfrei", Ventron, Karlsruhe, Germany) as a mineralizer [9]. The first analysis of single-crystal data obtained with Ag Kα radiation led to the NaCl structure type with a statistical occupation of all octahedral sites by nitrogen atoms [9]. This result is in contradiction to other X-ray powder investigations which describe occupation by nitrogen of a quarter of the octahedral sites in an ordered way. Therefore we collected new data with Mo Kα radiation on a single crystal of γ'-Fe_4N. The results of calculations confirm ordered occupation by nitrogen (Tables 1–3).

The single crystals we used contained about 5 wt.% Ni (EDX analysis) from the autoclave material (nickel-based alloy, DIN 2.4969). We suppose that nickel favours the crystallization of γ'-Fe_4N. Nevertheless we found no effect on crystallization caused by controlled addition of small amounts of nickel to the starting materials.

γ'-Fe_4N crystallizes in the $CaTiO_3$ structure type (perovskite), $Fe(2)NFe(1)_3$. Fig. 1 shows the unit cell. The arrangement of Fe(1) and Fe(2) can be described by the

☆ Dedicated to Professor P. Paetzold on the occasion of his 60th birthday.

SSDI 0925-8388(95)01610-4

Table 1
Technical and crystallographical data concerning structure determination of γ'-Fe_4N

Crystal size (mm^3)	$0.15\times0.15\times0.15$
Unit cell parameters (Å)	$a=3.7900(6)$
Volume (Å^3)	54.44
D_x (g cm^{-3})	7.242
Z	1
Space group	$Pm\bar{3}m$ (No. 221 [11])
$1/\mu$ (Mo Kα) (mm)	0.039
Absorption correction	None
Radiation	Mo Kα
Monochromator	Graphite
Scan mode	$\Omega/2\theta$
θ_{max} (deg)	60
h, k, l	$\pm9, \pm9, \pm9$
R_{merge} (%)	4.0
Independent reflections	137
Reflections with $F_o^2 \geq 3\sigma F_o^2$	59
Variables	6
R/R_w ($w=1$)	0.017/0.023
Extinction parameter	$2.48(3)\times10^{-5}$
Largest peak in the final difference map (e Å^{-3})	1.5

Table 2
Atomic coordinates and isotropic thermal displacement parameters (Å^2) for γ'-Fe_4N

Site	Atom	x	y	z	B
3d	Fe(1)	1/2	0	0	0.630(3)
1b	Fe(2)	1/2	1/2	1/2	0.373(5)
1a	N	0	0	0	0.42(3)

Table 3
Anisotropic thermal displacement parameters U_{ij} ($\times10^3$ Å^2) for γ'-Fe_4N

Atom	U_{11}	U_{22}	U_{33}	U_{12}	U_{13}	U_{23}
Fe(1)	4.9(2)	9.5(2)	U_{22}	0	0	0
Fe(2)	4.7(2)	U_{11}	U_{11}	0	0	0
N	5.0(10)	U_{11}	U_{11}	0	0	0

motif of undistorted cubic close packing (c.c.p.). Nitrogen occupies corner-sharing octahedra of Fe(1). This type of arrangement is the only possibility for maximum occupation of only corner-sharing octahedra in c.c.p. leading to the compositions $A_4B \triangleq \gamma'$-Fe_4N. The stacking sequence is $|A(Fe)_{\alpha(N)}B(Fe)_{\beta(N)}C(Fe)_{\gamma(N)}|\ldots$

3. Structure of ϵ-Fe_3N

3.1. Synthesis

We did not succeed in preparing iron nitrides with nitrogen content greater than 5.9 wt.% ($\triangleq Fe_4N$) by high pressure ammonolysis. Even the compounds Fe_3N or $Fe_3N_{1.25}$ as starting material decompose to γ'-Fe_4N and α-Fe.

For powder investigations of ϵ-Fe_3N we needed homogenous and pure samples. Therefore we decided to prepare iron nitride powders in a technical furnace (Carl Gommann, Remscheid, Germany) under normal nitridation conditions.

Samples of 100 g iron powder (Alfa, Karlsruhe, Germany, var. purities 99.9 and 99.999 wt.%) were treated with flowing ammonia (65 vol.% NH_3 and 35 vol.% decomposition products N_2 and H_2) at 510 °C and 1 bar total pressure. Cycles of 36 h duration were taken one to ten times. The furnace (volume approximately 50 m^3) was cooled down 50 °C per hour and from 400 °C to room temperature by substituting ammonia with nitrogen.

3.2. Structure determination

The obtained products always had the same analytical composition $Fe_3N_{0.99(1)}$ [2]. All Guinier diagrams were indexed on the basis of a hexagonal unit cell with the same refined cell parameters: $a=4.693(2)$ Å and $c=4.371(2)$ Å (Mo Kα_1 radiation, Guinier-Simon [12]).

For detailed structure analysis neutron powder diffraction data were collected at the DR3 reactor at Risø National Laboratory (Denmark) with the TAS1 instrument. The specimen was placed in a vanadium can of 8 mm diameter. Diffraction data were recorded at room temperature (298 K) and 609 K because of the ferromagnetism of ϵ-Fe_3N with $T_c=568$ K (Faraday balance). The step scan covered the angular range 5.0°–103.0° (for 298 K, 100.3°) in 2θ in steps of 0.1°. The wavelength of neutrons was 2.0129 Å.

The structure refinements were carried out with the program FULLPROF [13] based on the RIETVELD profile method [14] applying a Gaussian function. An initial refinement was made starting with the data proposed by Jack [8]. The ini-

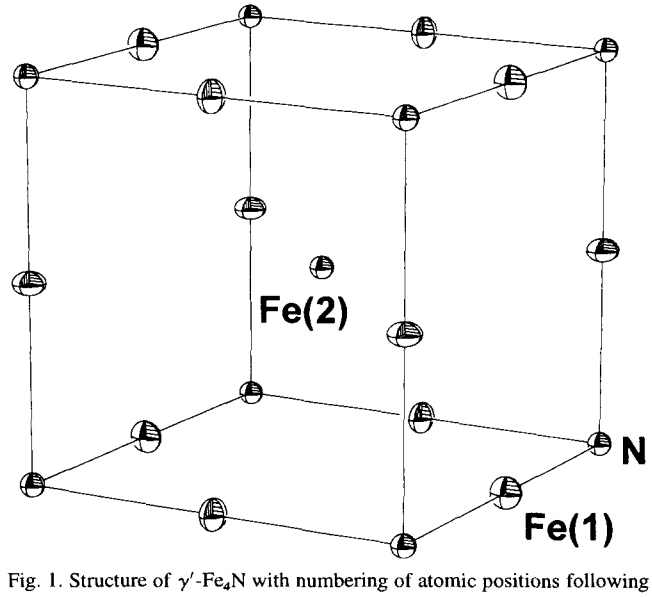

Fig. 1. Structure of γ'-Fe_4N with numbering of atomic positions following Table 1 as Fe(2)NFe(1)$_3$ within one unit cell. Ellipsoids of thermal vibrations of atoms are given for a reliability of 50%.

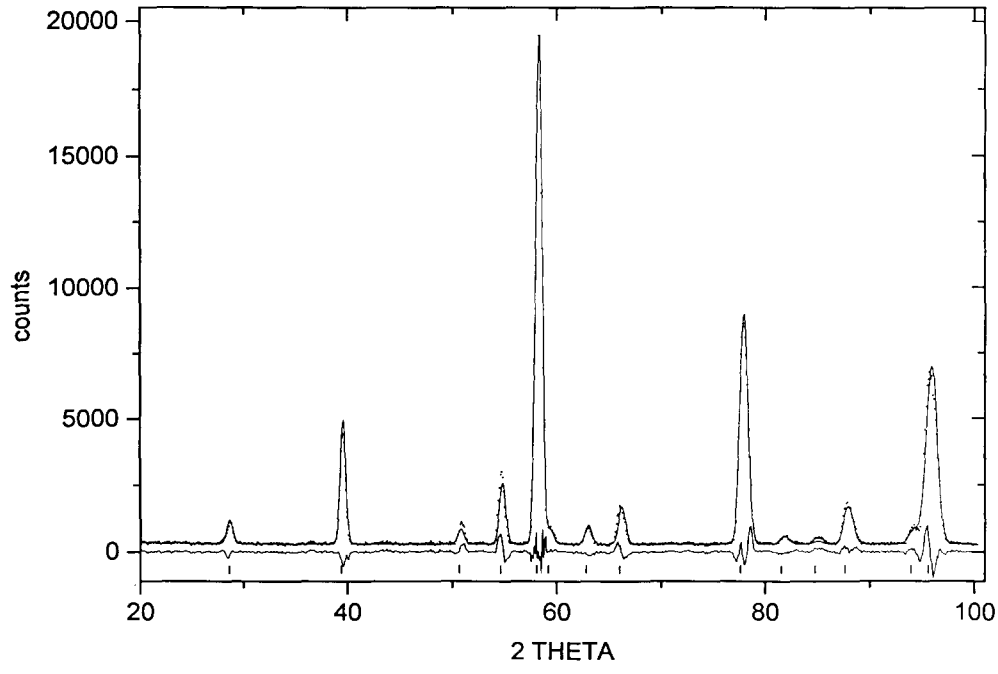

Fig. 2. Neutron diffraction diagram of ϵ-Fe_3N measured at room temperature (298 K) at TAS1 (Risø). Dotted curves give measured values, full lines give calculated values. A difference curve is shown below. The positions of reflections (vertical marks) are given (in the region from 5° to 20° in 2θ no reflection is observed).

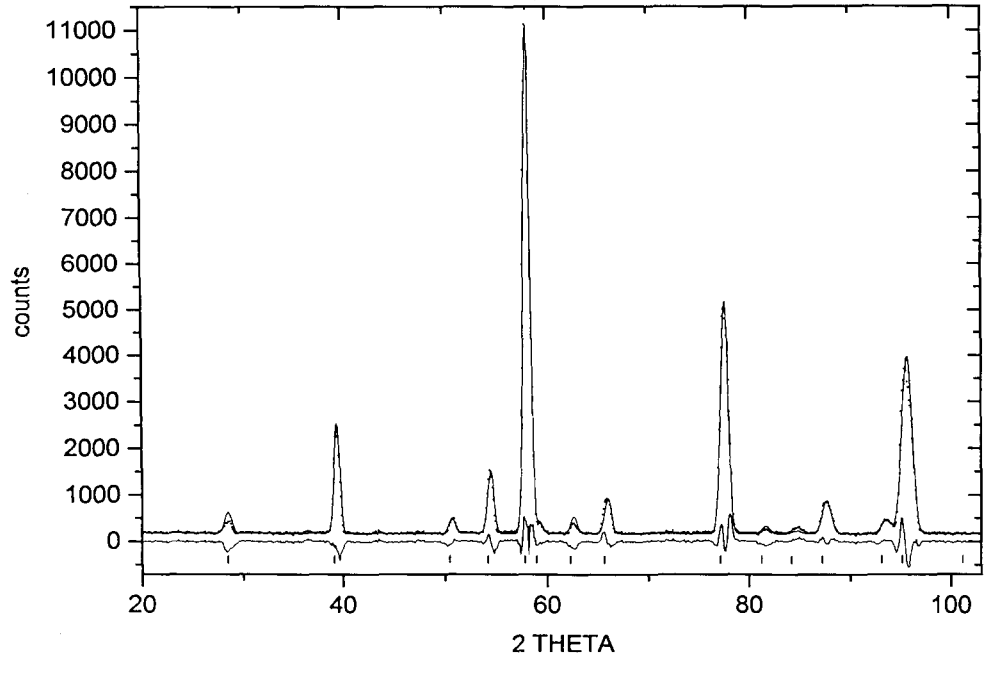

Fig. 3. Neutron diffraction diagram of ϵ-Fe_3N measured at 609 K at TAS1 (Risø). Dotted curves give measured values, full lines give calculated values. A difference curve is shown below. The positions of reflections (vertical marks) are given (in the region from 5° to 20° in 2θ no reflection is observed).

tially suggested space group $P312$ (No. 149 [11]) was modified to the minimal non-isomorphic supergroup $P6_322$ (No. 182 [11]) which includes all symmetry elements of Fe_3N. Satisfactory fits between observed and calculated neutron diffraction data of ϵ-Fe_3N for this refined model are illustrated in Fig. 2 (298 K) and Fig. 3 (609 K). Table 4 contains a comparison of the integrated observed and calculated intensities.

Both sets of diffraction data could be refined on the assumption of nuclear scattering only. Expected additional reflections and/or intensity changes giving information about the magnetic structure at 298 K could not be observed. To

Table 4
Neutron powder diffraction data of ϵ-Fe_3N (taken at Risø National Laboratory TAS1) at 298 K and 609 K, wavelength of neutrons 2.0129 Å

h k l	298 K			609 K		
	2θ	I_{obs}	I_{cal}	2θ	I_{obs}	I_{calc}
1 0 0	28.58	43	46	28.50	26	46
1 0 1	39.38	186	204	39.19	166	191
1 1 0	50.62	37	28	50.48	27	29
0 0 2	54.60	126	115	54.19	109	115
1 1 1	58.05	1000	996	57.82	1000	964
2 0 0	59.17	31	27	58.99	21	23
1 0 2	62.78	31	38	62.37	20	33
2 0 1	65.96	82	78	65.70	75	69
1 1 2	77.67	568	556	77.21	561	520
2 1 0	81.55	23	22	81.28	12	18
2 0 2	84.74	20	8	84.25	20	8
2 1 1	87.61	120	106	87.26	97	88
1 0 3	93.93	45	45	93.15	37	38
3 0 0	95.56	573	576	95.21	526	546
3 0 1				101.22	0	0

Table 5
Neutron powder diffraction data of ϵ-Fe_3N (taken at PSI, DMC) at 295 K and 9 K, wavelength of neutrons 1.7031 Å

h k l	295 K			9 K		
	2θ	I_{obs}	I_{calc}	2θ	I_{obs}	I_{calc}
1 0 0	24.16	40	43	24.19	39	42
1 0 1	33.20	188	210	33.27	183	204
1 1 0	42.51	33	25	42.57	34	25
0 0 2	45.78	138	111	45.91	141	110
1 1 1	48.58	1000	972	48.67	1000	967
2 0 0	49.49	35	31	49.56	35	30
1 0 2	52.42	34	42	52.56	33	41
2 0 1	54.97	71	81	55.07	70	80
1 1 2	64.24	542	541	64.39	544	545
2 1 0	67.25	20	24	67.35	19	23
2 0 2	69.69	5	7	69.85	5	7
2 1 1	71.87	106	111	72.00	106	111
1 0 3	76.60	49	46	76.84	47	46
3 0 0	77.79	523	523	77.91	539	540
3 0 1	82.19	0	0	82.33	0	0
2 1 2	85.17	21	20	85.36	22	21
1 1 3	86.76	400	402	87.02	421	423
2 0 3	91.78	36	36	92.05	37	37
2 2 0	92.94	8	9	93.10	10	10
3 0 2	95.22	221	232	95.44	241	252
2 2 1	97.29	348	355	97.48	374	381
3 1 0	97.98	3	3	98.16	3	3
0 0 4	102.13	136	133	102.52	147	142
3 1 1	102.39	71	69	102.59	74	72
2 1 3	107.09	73	68	107.42	77	71
1 0 4	107.32	7	7	107.74	7	7
2 2 2	110.72	303	286	110.99	325	309
4 0 0	113.68	0	0	113.92	0	0
3 1 2	116.19	40	46	116.49	44	48
3 0 3	117.98	0	0	118.36	0	0
1 1 4	118.23	17	18	118.70	21	22
4 0 1	118.51	28	30	118.78	29	32
2 0 4	124.10	22	20	124.62	24	21

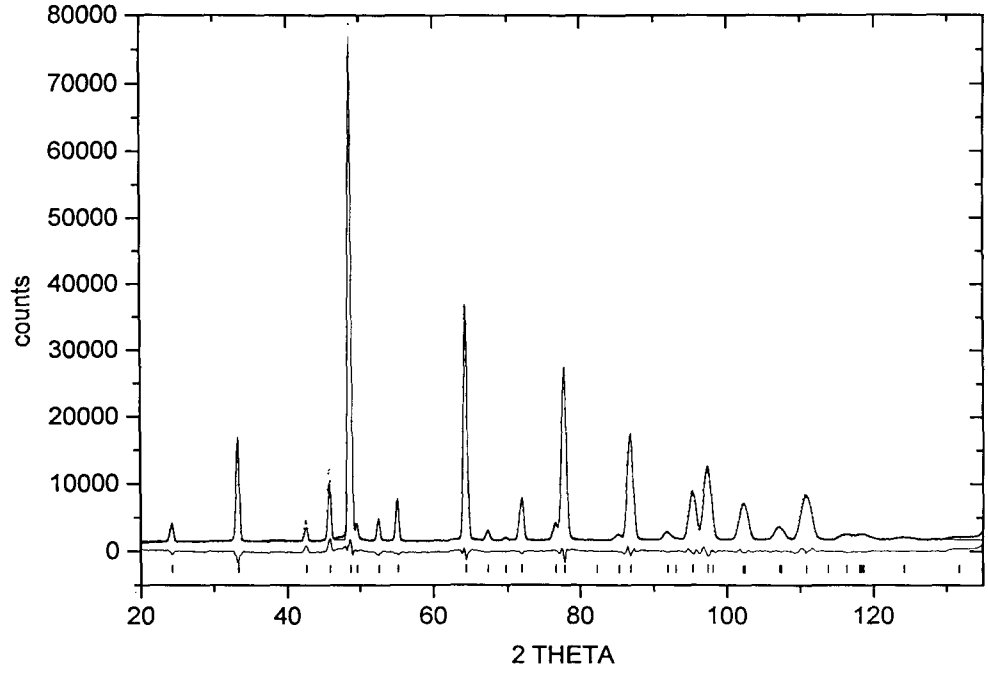

Fig. 4. Neutron diffraction diagram of ϵ-Fe_3N measured at room temperature (295 K) at DMC (PSI). Dotted curves give measured values, full lines give calculated values. A difference curve is shown below. The positions of reflections (vertical marks) are given (in the region from 3° to 20° in 2θ no reflection is observed).

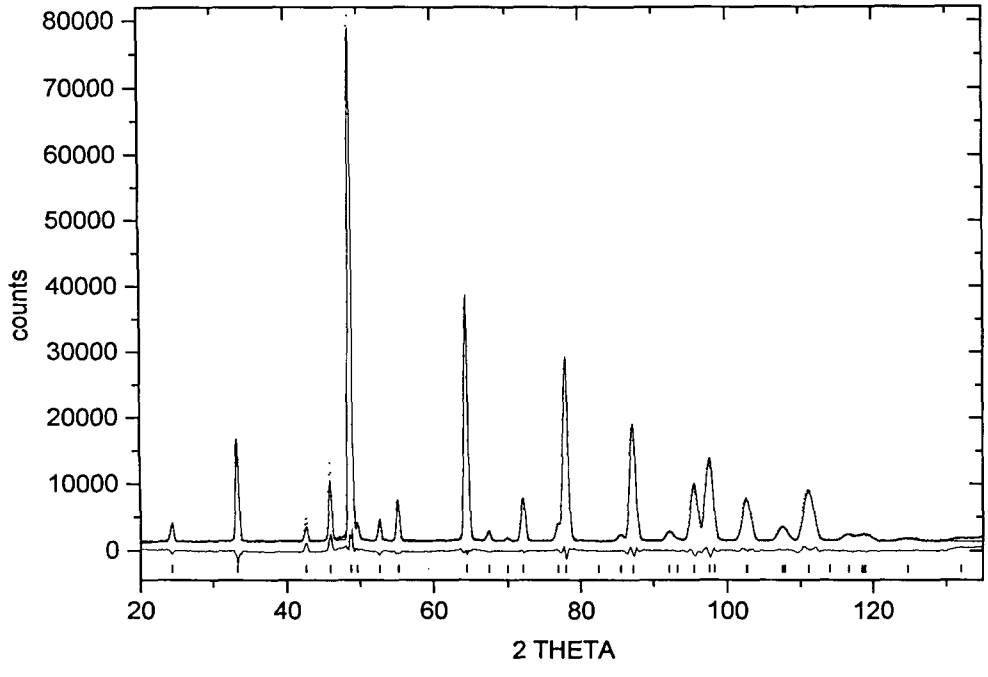

Fig. 5. Neutron diffraction diagram of ϵ-Fe_3N measured at 9 K at DMC (PSI). Dotted curves give measured values, full lines give calculated values. A difference curve is shown below. The positions of reflections (vertical marks) are given (in the region from 3° to 20° in 2θ no reflection is observed).

prove the supposition that the magnetic spins have low ordered orientation because of high temperature motion, we took diffraction data down to 9 K (Saphir, Paul-Scherrer Institut (PSI), Switzerland) without and in a magnetic field (Orphée, Saclay Laboratoire Leon Brillouin, France). Up to now no influence on the intensities of the reflections caused by magnetic ordering could be observed.

Hence we propose, in analogy with α-Fe, a band-magnetism which cannot be observed by standard elastic neutron diffraction techniques [15]. Further investigations of the

Table 6
Structural and profile refinement parameters of ϵ-Fe_3N, neutron diffraction data were taken at Risø National Laboratory (TAS1) and Paul-Scherrer Institut (DMC), for further information see text

Space group $P6_322$ (No. 182 [11]), $Z=2$; 6Fe in site 6g x, 0, 0; 2N in site 2c 1/3, 2/3, 1/4

	TAS1	TAS1	DMC	DMC
Temperature (K)	609	298	295	9
Wavelength (Å)	2.0129	2.0129	1.7031	1.7031
2θ range (deg) (step 0.1°)	5.0–103.0	5.0–100.3	3.0–134.9	3.0–134.9
Number of reflections	15	14	34	35
Number of structural parameters	5	5	5	5
Cell parameters				
a (Å)	4.7209(6)	4.7080(6)	4.6982(3)	4.6919(4)
c (Å)	4.4188(9)	4.3885(9)	4.3789(4)	4.3670(4)
$\sqrt{3}c/a$	1.621	1.615	1.614	1.612
Volume (Å^3)	85.29	84.24	83.71	83.26
Reliability factors				
R_{Bragg} (%)	7.44	3.59	4.14	4.31
$R_{Profile}$ (%)	9.54	8.47	4.43	4.68
R_{wp} (%)	13.10	11.70	6.05	6.51
R_{exp} (%)	3.97	2.86	1.53	1.53
x(Fe)	0.3278(7)	0.3264(7)	0.3249(4)	0.3250(4)
B(Fe) (Å^2)	0.3(1)	0.4(1)	0.40(3)	0.13(3)
B(N) (Å^2)	1.9(1)	1.4(1)	0.81(5)	0.65(5)

Table 7
Distances (Å) and angles (deg) for γ'-Fe_4N and ϵ-Fe_3N, with α-Fe for comparison; standard deviations including deviations in cell parameters

	α-Fe [16]	γ'-Fe_4N	ϵ-Fe_3N
Fe–Fe	8×2.482	12×2.680(1)	2×2.644(2)
	6×2.866		4×2.669(1)
	(12×2.57) [a]		2×2.739(2)
			4×2.748(2)
N–Fe:		6×1.895(1)	6×1.927(1)
N–N		6×3.790(1)	6×3.486(1)
Fe–N–Fe		12×90	3×87.76(5)
			3×90.49(6)
			6×90.89(6)
		3×180	3×178(3)
N–Fe–N		180	129.47(7)

[a] Distance for hypothetical γ'-Fe approximated by the equation (after [17]) $R_{CN12}=(1.0316R_{CN8}+0.532)$ pm).

magnetic behaviour and the magnetic structure of ferromagnetic ϵ-Fe_3N are in progress.

The data collections on DMC at the Saphir-reactor (Paul-Scherrer Institut (PSI), Switzerland) at 295 K and 9 K were done in the high intensity mode. The wavelength of neutrons was 1.7031 Å. The step scan covered the angular range 3.0°–134.9° in 2θ in steps of 0.1°. For comparison with Risø measurements we performed further profile analysis. Figs. 4 (295 K) and 5 (9 K) show observed and calculated neutron diffraction data and Table 5 gives a comparison of integrated intensities.

3.3. Results and discussion

Table 6 shows structural parameters of ϵ-Fe_3N at 609 K (Risø), 298 K (Risø), 295 K (PSI) and 9 K (PSI). The refinements led to good reliability factors $R_{Profile}$ and R_{Bragg}. The higher R value for the 609 K refinement is affected by short recording times and consequently bad intensity-to-background ratio. Nevertheless all parameters derived from these different measurements show very good agreement.

In ϵ-Fe_3N the iron atoms show the motif of a slightly distorted hexagonal close packing (h.c.p.) structure. Nitrogen atoms occupy only corner-sharing octahedra. Here we find again a maximum occupation of only corner-sharing octahedra by nitrogen atoms in h.c.p. iron as in γ'-Fe_4N for c.c.p. iron.

All iron atoms have two nitrogen neighbours. The structure of ϵ-Fe_3N is illustrated in Fig. 6(b) in comparison with the structure of γ'-Fe_4N (Fig. 6(a)).

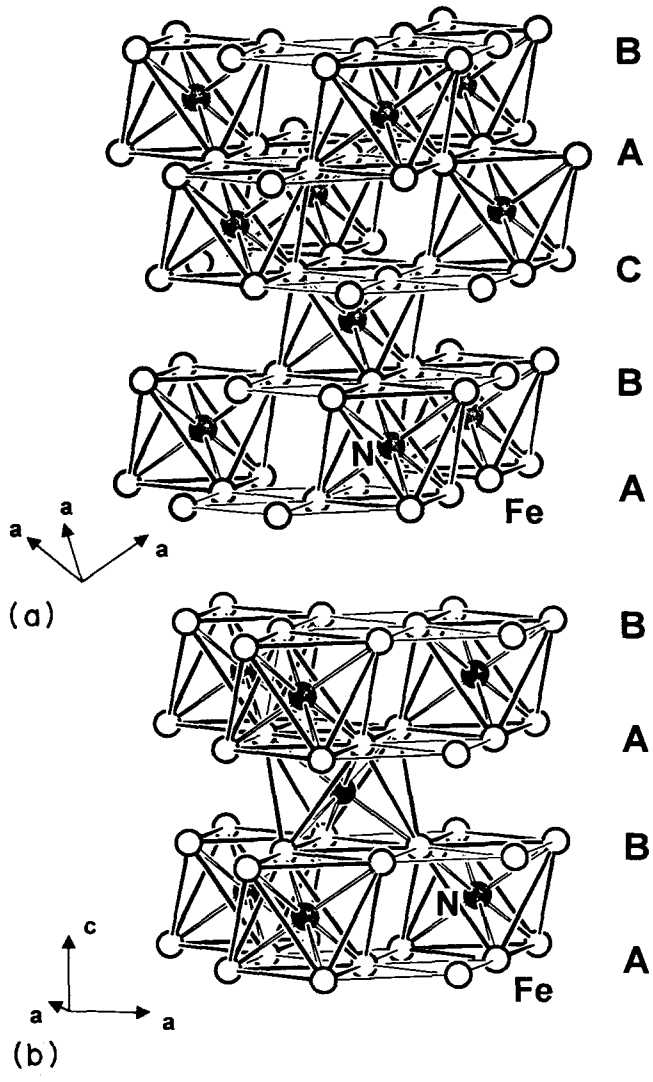

Fig. 6. Comparison of the atomic arrangements in γ'-Fe_4N and ϵ-Fe_3N. (a) γ'-Fe_4N described by a cubic sequence |ABC| of close packed iron layers with nitrogen in only corner-sharing octahedral sites; (b) ϵ-Fe_3N described by an analogous graph for a hexagonal close packed sequence |AB|.

In ϵ-Fe_3N the occupation of only corner-sharing iron octahedra is the simplest solution with shortest periodicity in the c direction. The stacking sequence is $|A(Fe)_{\alpha(N)}$-$B(Fe)_{\beta(N)}|$...

The distortion of the h.c.p. arrangement of iron is small. The ratio $\sqrt{3}c/a = 1.614$ at room temperature is near the ideal value for h.c.p.: $c/a = \sqrt{(8/3)} \approx 1.633$. Furthermore the shift of the x-parameter of iron atoms differs less than 0.009 (ideal $x = 1/3$). Table 7 gives interatomic distances and angles. The Fe–Fe distance in b.c.c. α-Fe increases up to about 8% by insertion of nitrogen atoms into γ'-Fe_4N. Here we have a regular cuboctahedron of iron atoms with 12 equal distances. Further insertion of nitrogen leads to a slightly distorted anti-cuboctahedron in ϵ-Fe_3N. The distances d(Fe–Fe) are now significantly divided into two values: 6×2.66 Å and 6×2.74 Å. The average of 2.70 Å is nearly the same as in γ'-Fe_4N. The bond angle N–Fe–N becomes 129.5° instead of 131.8° for the ideal h.c.p. structure. An anti-cuboctahedron of iron atoms with sharing Fe_6N octahedra is shown in Fig. 7.

We measured the pycnometric density of ϵ-Fe_3N (gas displacement pycnometer, AccuPyc 1330, micromeritics, Neuss, Germany) and found $\rho_{exp} = 7.164(1)$ g cm^{-3}. This value is in good agreement with the calculated density $\rho_{neutron} = 7.204$ g cm^{-3}. Mössbauer spectroscopic investigations by Mittemeijer and Somers [18] on the sample used here show nearly perfect ordering of nitrogen.

The c/a ratio approximates the ideal value with rising temperatures (c.f. Table 6). We supposed a weak ferromagnetic coupling in the z-direction which should lead to a contraction of the cell parameter c. Robbins and White [19] propose an orientation of magnetic spins parallel to c. Their neutron powder investigations showed few changes in intensity. Our measurements did not verify these results.

Our knowledge of the phase diagram Fe–N regarding the structures of nitride phases determined so far is as follows. In the α-Fe phase nitrogen is randomly distributed in strongly distorted iron octahedra with a maximum solubility of 0.1 wt.% N at 550 °C [20]. Up to about 5.9 wt.% N the two-phase region (α-Fe and γ'-Fe_4N) exists. In γ'-Fe_4N the iron atoms are rearranged from b.c.c. to c.c.p. with nitrogen atoms ordered in corner-sharing octahedra only. Further insertion of nitrogen atoms would lead at least to edge-sharing occupied iron octahedra. This means that nitrogen atoms come closer to one another. Therefore the iron substructure is reorganized to h.c.p. with only corner-sharing octahedra in ϵ-Fe_3N with about 7.7 wt.% N. In our opinion the inserted nitrogen forces the arrangement of iron according to electrostatic principles in such a way that the nitrogen atoms have the maximal possible distances between one another. Therefore the compositions γ'-Fe_4N (c.c.p.) and ϵ-Fe_3N (h.c.p.) are thermodynamically preferred with respect to the occupation of only corner-sharing octahedra. This view is clearly driven by electrostatic aspects. Both nitrides are metallic ferromagnets and show only small distortions in the iron substructure. The calculation of volume increments leads to such values for nitrogen that one cannot discuss nitride ions N^{3-} within γ'-Fe_4N and ϵ-Fe_3N. The main part of the chemical bonding between iron and nitrogen must be covalent in nature.

Acknowledgements

We thank the "Bundesminister für Forschung und Technologie" (BMFT, Contract No. 03-JA2DOR) for financial support. Many thanks for enthusiastic help in the preparation of iron nitride samples to Dipl.-Ing. U. Huber-Gommann (Härterei Carl Gommann, Remscheid, Germany). For recording neutron diffraction data we thank Dr. P. Müller (Inorganic Chemistry, RWTH Aachen, Germany), Dr. P. Fischer (PSI Wuerenlingen, Switzerland) and Dr. W. Paulus (Saclay Laboratoire Leon Brillouin, Gif-sur-Yvette, France).

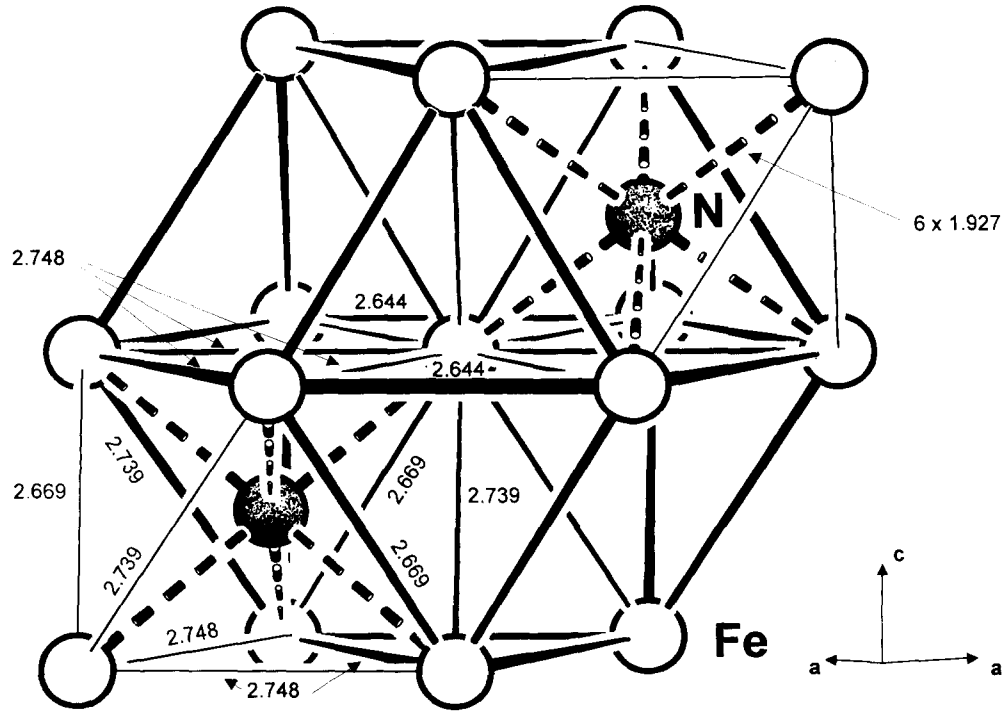

Fig. 7. Anti-cuboctahedron of Fe in ϵ-Fe_3N with sharing nitride occupied Fe_6N-octahedra. Distances d(Fe–Fe) and d(Fe–N) are given in Ångströms.

References

[1] B. Prenosil, *Härterei-Tech. Mitt., 28* (1973) 157.
[2] H. Jacobs, D. Rechenbach and U. Zachwieja, *Härterei-Tech. Mitt.*, in press.
[3] G. Hägg, *Nature, 121* (1928) 826.
[4] S.B. Hendricks and P.R. Kosting, *Z. Kristallogr., 74* (1930) 511.
[5] R.J. Bouchard, C.G. Frederick and V. Johnson, *J. Appl. Phys., 45* (1974) 4067.
[6] K.H. Jack, *Proc. R. Soc. London, Ser. A, 195* (1948) 34.
[7] K.H. Jack, *Acta Crystallogr., 3* (1950) 392.
[8] K.H. Jack, *Acta Crystallogr., 5* (1952) 404.
[9] H. Jacobs and J. Bock, *J. Less-Common Met., 134* (1987) 215.
[10] H. Jacobs and D. Schmidt, in E. Kaldis (ed.), *Current Topics in Materials Science*, Vol. 8, North-Holland, Amsterdam, 1981, p. 379.
[11] T. Hahn (ed.), *International Tables for Crystallography*, Vol. A, *Space Group Symmetry*, Kluwer, Dordrecht, 1992.
[12] A. Simon, *J. Appl. Crystallogr., 3* (1970) 11.
[13] J. Rodriguez-Carvajal, *Program FULLPROF, Version 2.4.2.*, December 1993 (Institut Laue-Langevin (ILL)).
[14] D.W. Wiles and R.A. Young, *J. Appl. Crystallogr., 14* (1981) 149.
[15] G.E. Bacon, *Neutron Diffraction*, Clarendon Press, Oxford, 1975, 3rd edn.
[16] R. Kohlhaas, P. Dünner and N. Schmitz-Prange, *Z. Angew. Phys., 23* (1967) 245.
[17] R. Ferro and A. Saccone, in R.W. Cahn, P. Haasen and E.J. Kramer (eds.), *Materials Science and Technology*, Vol. 1, Verlag Chemie (VCH), Weinheim, 1993, p. 123.
[18] E.J. Mittemeijer and M.A.J. Somers, unpublished results, Delft University of Technology.
[19] M. Robbins and J.G. White, *J. Phys. Chem. Solids, 25* (1969) 717.
[20] H.A. Wriedt, N.A. Gokcen and R.H. Nafziger, *Bull. Alloy Phase Diagrams, 8* (1987) 355.